Available online at www.sciencedirect.com
ScienceDirect
Polymer 47 (2006) 6501–6508
polymer
www.elsevier.com/locate/polymer

High molecular weight methyl ester of microbial poly(β,L-malic acid): Synthesis and crystallization

Carlos E. Fernández [a], Manuel Mancera [b], Eggehard Holler [c], Juan A. Galbis [b,*], Sebastián Muñoz-Guerra [a,*]

[a] *Departamento d'Enginyeria Química, Universitat Politècnica de Catalunya, ETSEIB, Diagonal 647, Barcelona 08028, Spain*
[b] *Departamento de Química Orgánica y Farmacéutica, Universidad de Sevilla, Sevilla 41071, Spain*
[c] *Institut für Biophysik und Physikalische Biochemie der Universität, D-93040, Regensburg, Germany*

Received 29 May 2006; received in revised form 20 July 2006; accepted 26 July 2006
Available online 14 August 2006

Abstract

High molecular weight poly(α-methyl β,L-malate) ($M_n \sim 25{,}000$, PD ~ 1.7) was prepared from microbial poly(β,L-malic acid) ($M_n \sim 29{,}000$, PD ~ 1.3) by methylation with diazomethane in dry acetone without substantial cleavage of the polyester main chain. The thermal properties of this poly(malate) were assessed and its crystal structure was preliminary examined. Two crystal forms were identified by X-ray diffraction, their occurrence being dependent on crystallization conditions. The kinetics of nonisothermal and isothermal crystallizations from the melt were studied and modelled using the Avrami approach. Results were compared to those recently reported by us for low molecular weight poly(α-methyl β,L-malate) ($M_n \sim 3000$, PD ~ 1.3).

Keywords: Poly(malic acid); Poly(malate); Biotechnological polyester

1. Introduction

Poly(β-malic acid) (PMLA) is a polyester composed of malic acid (α-hydroxy succinic acid) units that are linked by an ester bond formed between the hydroxyl group and the carboxyl group located at the β position. This polymer is highly water-soluble, biodegradable, nonimmunogenic and nontoxic, and it is metabolized in the mammalian tri-carboxylic acid (TCA) cycle [1]. PMLA and its derivatives have continuously attracted scientific and technological attention for their potential as materials usable for temporary biomedical applications [2]. The polyacid can be modified at the pendant carboxyl group allowing the covalent attachment of drugs to the polymer chain. A prototype of a polyfunctional nanoconjugate for targeted delivery of antisense oligonucleotides and monoclonal antibodies to brain tumours has been recently developed using microbial PMLA [3]. Stoichiometric ionic complexes of PMLA with cationic surfactants displaying nanostructured amphiphilic phases have been recently reported [4].

Poly(β-malic acid) can be chemically synthesized or biosynthetically produced by certain myxomycetes and filamentous fungi. Direct polycondensation of malic acid invariably leads to heterogeneous polymers consisting of mixtures of α and β-malate units and molecular weights lower than 3000 [5]. It was the successful synthesis of benzyl malolactonate achieved in 1979 [6] that made possible the access to synthetic PMLA of high molecular weight. Today both racemic and optically pure (either D or L) compounds can be obtained by chemical synthesis [7]. In contrast, the polyacid of microbial origin is enantiomerically pure and may attain molecular weights of hundreds of thousands [1]. Modification of the carboxylic side group of poly(β-malic acid) requires the use of highly specific reactions that do not affect the easily breakable

* Corresponding authors.
E-mail addresses: jgalbis@us.es (J.A. Galbis), sebastian.munoz@upc.edu (S. Muñoz-Guerra).

0032-3861/$ - see front matter © 2006 Published by Elsevier Ltd.
doi:10.1016/j.polymer.2006.07.063

main chain ester bond. A wide variety of derivatives are potentially accessible by chemical coupling. However, a complete conversion is difficult to reach without substantial decrease of the initial molecular weight.

Esterification of the carboxyl side group of water-soluble polycarboxylic polymers, as it is in the case of poly(β-malic acid), usually renders polymers with the original properties dramatically changed. Recently we have reported on the synthesis of poly(α-methyl β,L-malate) (PAALM-1) by reaction of biosynthetic PMLA with diazomethane in dimethyl sulphoxide [8]. Although this method was proven to be efficient to prepare 100% esterified PMLA, substantial cleavage of the main chain could not be avoided so that a poly(malate) of M_n approximately 3000 was obtained from a sample of PMLA of M_n approximately 30,000. Such low molecular weight poly(malate) was described as a nonwater-soluble polymer melting at approximately 140 °C without decomposition and exhibiting a high degree of crystallinity. In this paper we report on a poly(α-methyl β,L-malate) with a M_n about 10 times higher than that has been prepared from PMLA of the same microbial source. It is named PAALM-1(HMW) to be distinguished from the low molecular homologous PAALM-1(LMW). Our investigation complements that carried out previously on PAALM-1(LMW) by evaluating the influence of the molecular size on the crystal structure, thermal properties and crystallization behaviour. While crystallization kinetic studies of PAALM-1(LMW) were not possible due to the extremely slow rate of crystallization from the melt displayed by this polymer, PAALM-1(HMW) crystallizes from the melt at DSC measurable rates allowing the study of the crystallization kinetics under both isothermal and nonisothermal conditions.

2. Materials and methods

Poly(β,L-malic acid) was obtained by cultivation of the myxomycete *Physarum polycephalum* according to a previously reported method [9]. The esterification reaction of PMLA was performed as follows: to a solution of the polyacid (500 mg, 4.3 mequiv) in dried acetone (25 mL), a solution of diazomethane in ether (50 mL, 12.5 mequiv) was added, and the mixture left under stirring at room temperature for 1 h. Evaporation under vacuum rendered PAALM-1 as a white powder, which was then washed with ether (150 mL) and dried. The methylated compound was obtained as a white powder in 90% yield. ^{1}H and ^{13}C NMR spectra were recorded on a Bruker AMX-300 NMR instrument with samples dissolved in $CDCl_3$ either pure or added with trifluoroacetic acid, and using TMS as internal reference. Sample concentrations of about 1% (w/v) were used for this analysis. Viscosimetry measurements were made in a Ubbelhode viscometer thermostated at 25 °C. Gel permeation chromatography was carried out in hexafluoroisopropanol (HFIP) containing 0.05 M sodium trifluoroacetate and molecular weights were absolutely estimated by light scattering (LS). The specific refractive index increment (dn/dc) for PAALM-1 in the fluorinated solvent was determined at 35 °C in an Optilab refractometer from Wyatt to be 0.160 mL/g. The thermal stability of PAALM-1 was analyzed by thermogravimetry (TGA) and its thermal transitions and crystallization kinetics were analyzed by differential scanning calorimetry (DSC). TGA measurements were performed with a TGA-6 Perkin–Elmer thermobalance under inert atmosphere using 15–20 mg sample weights. DSC measurements were carried out under circulating nitrogen on a Perkin–Elmer Pyris 1 calorimeter calibrated with indium. DSC data were obtained from samples of 4–6 mg weight. Glass transition temperatures were measured at a heating rate of 20 °C/min from samples quenched from the melt. Both isothermal and nonisothermal crystallizations were carried out from samples molten at 200 °C and NMR and GPC analysis of crystallized samples did not show evidences of thermal degradation. Polarizing optical microscopy (POM) was performed using an Olympus BX51 microscope with a digital camera attached. A hot-stage Linkam THMS 600 provided with a N_2 cooling system was used for crystallizations performed under the optical microscope. Crystallized films were obtained by melting the polymer between two microscope cover slides for 5 min followed by quickly cooling to the chosen temperature. X-ray diffraction patterns were obtained with a modified Statton camera using Nickel-filtered Cu Kα radiation of wavelength 0.1542 nm, and they were calibrated with molybdenum sulphide (d_{002} = 0.6147 nm).

3. Results and discussion

3.1. Synthesis and characterization

The crude sample of poly(β,L-malic acid) produced by fermentation was subjected to fractionation over Sephadex G25. The fraction collected for this study was proven to be spectroscopically pure by NMR analysis, and to have a number-average molecular weight around 30,000 with a polydispersity close to 1.25. Esterification with diazomethane in solution at room temperature produced PAALM-1 in about 90% yield (Scheme 1) with a conversion of 100% and no detectable secondary reactions. However, the molecular size of the resulting PAALM-1 was found to be highly dependent on the solvent in which the esterification reaction was carried out. The ^{1}H NMR spectra of PAALM-1 obtained in DMSO and acetone, are compared in Fig. 1. The minor peak at 3.7 ppm observed in the spectrum of PAALM-1 obtained in DMSO corresponds to the methyl side group of the β-malate chain end unit. A number-average molecular weight of about 3000 was estimated for this PAALM-1 sample by comparing the area of this peak with that of the peak at 3.8 ppm arising from interior methyl groups. Conversely, no end group peak is observed in the spectrum of PAALM-1 that was prepared

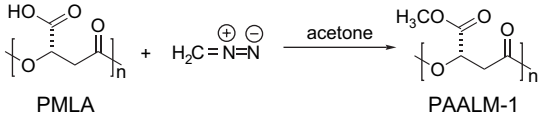

Scheme 1.

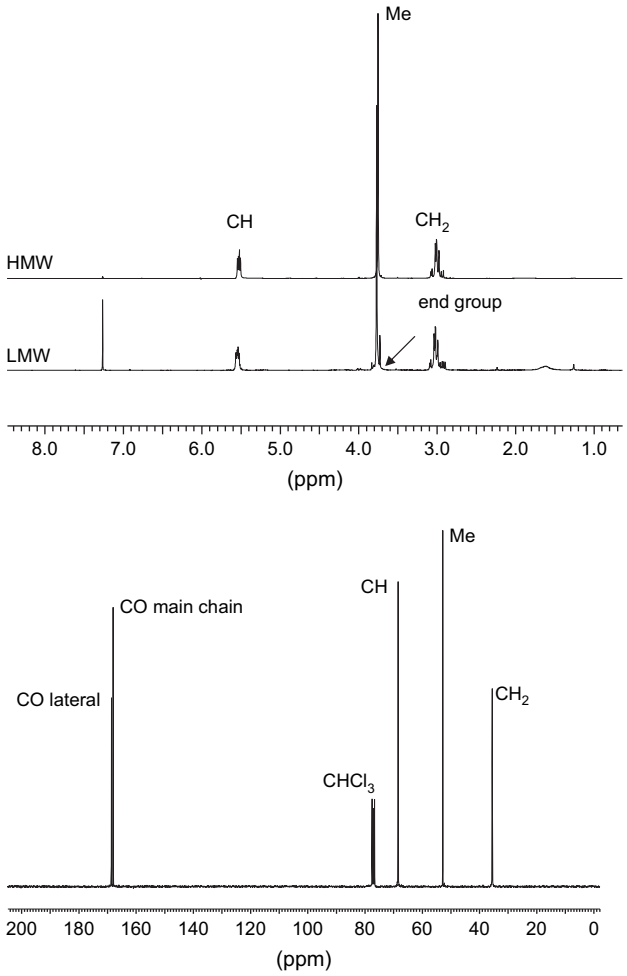

Fig. 1. ^{1}H NMR spectra of LMW and HMW PAALM-1 (top) and ^{13}C NMR (bottom) spectra of PAALM-1(HMW).

using acetone as solvent in the esterification reaction, indicating that much higher molecular size had been obtained by this method. In fact, GPC analysis of these two samples performed under the same conditions revealed that the M_n of PAALM-1 obtained in acetone was about 10 times higher, which is the expected value in the absence of main chain cleavage. This dramatic difference in results is explained taking into account the extreme sensitivity of the polymalic chain to hydrolysis. Small amounts of water present in hydrophilic solvents such as DMSO, which are irremovable by standard methods, will be able to degrade significantly the polyester chain. It is calculated that the degradation observed in DMSO resulted from the hydrolysis of about one of every 10 main chain ester bonds, which would require only 1–2% (w/w) of water present in the reaction medium.

The thermal behaviour of PAALM-1 was evaluated by TGA and DSC. PAALM-1s, (LMW) and (HMW), started to decompose at temperatures well above 200 °C leaving a few percent of residual material. In Fig. 2, the TGA traces of the polyacid and the low and high molecular weight PAALM-1s are compared. Whereas differences between PMLA and PAALM-1(LMW) traces are not detectable, the trace of PAALM-1(HMW) is displaced toward higher temperatures

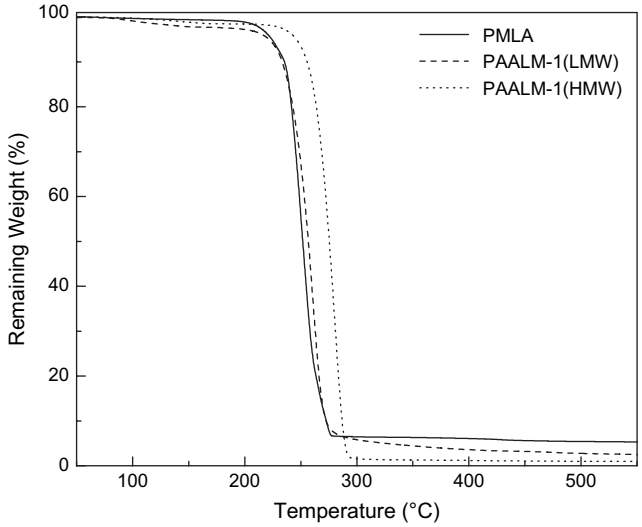

Fig. 2. TGA traces of PMLA and PAALM-1 of low and high molecular weight.

indicating a significant increase in the thermal stability with molecular weight. It has been recently found that thermal degradation of PMLA takes place by an unzipping depolymerization mechanism process that initiates at the carboxylic end groups of the polymer [10]. On the contrary, PAALM-1 degrades by a main chain scission process based on an α,β-elimination reaction similar to that reported for poly(hydroxy butyrate) [11]. Since PAALM-1 is completely methylated, the influence of the molecular size on the thermal stability of PAALM-1 is explainable in terms of main chain mobility rather than by end group effect.

The DSC traces characterizing the basic thermal behaviour of PAALM-1(HMW) are depicted in Fig. 3. They show that this polymer melts and crystallizes reversibly at temperatures between 100 and 150 °C, closely resembling the behaviour shown by other aliphatic polyesters such as poly(β-hydroxy butyrate)

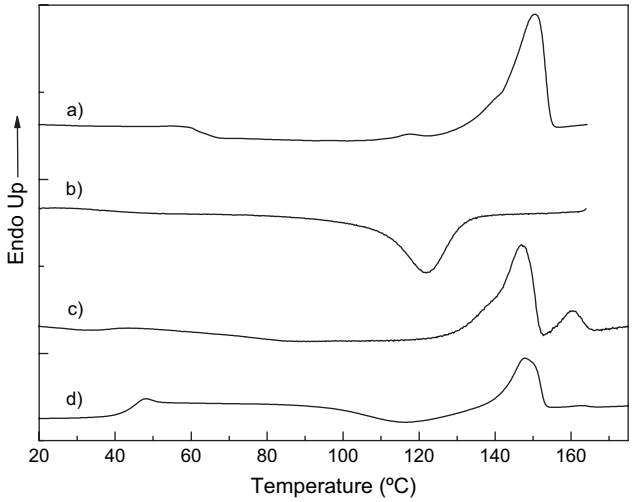

Fig. 3. DSC traces of PAALM-1(HMW): (a) first heating, (b) cooling at 10 °C/min, (c) second heating, and (d) heating trace of a sample quenched from the melt.

Table 1
Characteristics of poly(β,L-malic acid) and poly(α-methyl β,L-malate)s studied in this work

Synthesis[a]		DSC[b]			TGA[c]			η[d]	GPC[e]	
		T_m (°C)	ΔH_m (J/g)	T_g (°C)	T_d^0 (°C)	T_d (°C)	ΔW (%)	–	M_w	M_n
PMLA	*P. polycephalum*	216	42	110	236	250	5.3		36,200	29,000
PAALM-1(LMW)	DZM/DMSO	137	21	38	233	260	2.5	0.13	3600	2900
PAALM-1(HMW)	DZM/acetone	151	42	41	256	280	1.0	0.29	42,900	24,500

[a] Method of synthesis (DZM: diazomethane; DMSO: dimethyl sulphoxide).
[b] Melting (T_m) and glass transition (T_g) temperatures and fusion enthalpy ΔH_m measured by DSC for samples freshly synthesized.
[c] Onset (T_d^0) and maximum rate (T_d) decomposition temperatures and remaining weight (ΔW) measured by TGA.
[d] Reduced viscosity measured in $CHCl_3$ (1% w/v) at 25 °C.
[e] Weight-average (M_w) and number-average (M_n) molecular weights measured by GPC with light scattering detection.

[12]. Whereas a single endothermic peak is observed in the heating scan of the powder sample coming from synthesis, two melting peaks appeared in the second heating trace recorded from samples crystallized from the melt. On the other hand, the glass transition was clearly evidenced on the heating trace obtained from a sample that was solidified by cooling rapidly from the melt. Thermal parameters measured by TGA and DSC for both high and low molecular weight PAALM-1s are compared in Table 1. A significant increase in all the listed thermal parameters is observed for PAALM-1(HMW).

3.2. Crystal structure

The X-ray diffraction analysis assessed the semicrystalline nature of PAALM-1 previously evidenced by DSC. The intensity scattering profiles of PAALM-1(HMW) and PAALM-1(LMW) recorded from samples coming from synthesis are compared in Fig. 4 and the Bragg spacings measured in the original photographs are listed in Table 2. These results do not show significant differences between the low and high molecular weight samples. In both cases highly crystalline patterns consisting of more than a dozen of sharp rings coinciding in spacings and intensities were obtained. The structure present in these samples (form I) is characterized by two strong reflections at 6.9 and 5.9 Å and a melting temperature of 150 °C. On the other side, the X-ray diffraction analysis of the higher temperature peak (close to 160 °C) observed in the DSC trace of PAALM-1(HMW) crystallized from the melt (Fig. 3), revealed that it corresponds to a second crystalline structure (form II) characterized by two strong reflections at 8.1 and 6.2 Å. Besides these differences, most of all other reflections are shared by the two forms. Unfortunately, oriented samples of PAALM-1 which had allowed performing a detailed structural analysis could not be prepared due to technical reasons. Nevertheless, the results obtained so far indicate that PAALM-1(HMW) is able to crystallize in two closely related crystal forms, both of them presumably made of chains in a regularly folded conformation similar to that described for poly(β-hydroxy butyrate), a polyester with the same backbone constitution [13].

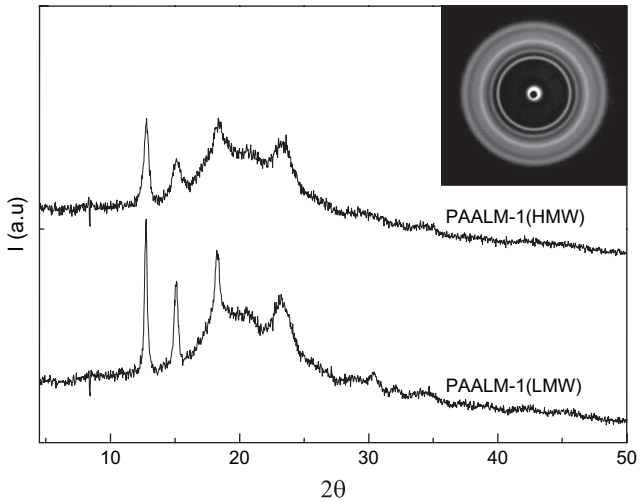

Fig. 4. WAXS profiles of PAALM-1. Inset: powder diffraction pattern of PAALM-1(HMW).

3.3. Nonisothermal crystallization

The DSC traces of the nonisothermal crystallization of PAALM-1(HMW) taken at different cooling rates together with the heating DSC traces of the respective crystallized samples are shown in Fig. 5. It is observed that the crystallization

Table 2
Diffraction spacings (Å) of PAALM-1

PAALM-1 (synthesis powder)[a]		PAALM-1(HMW) (crystallized from the melt)[b]	
(LMW)	(HMW)	135 °C	150 °C
		8.20 w	8.20 m
6.94 s	6.94 s	6.94 s	
		6.26 w	6.26 m
5.87 s	5.87 s	5.81 s	
4.85 s	4.85 s	4.80 s	4.80 s
4.31 m	4.31 m	4.26 m	4.26 m
3.83 s	3.83 s	3.73 s	3.77 s
		3.33 w	3.33 m
3.09 w	3.09 w		3.12 w
2.93 w	2.93 w	2.92 w	2.88 w
2.78 w	2.78 w	2.77 w	2.75 w
2.62 w	2.62 w		2.62 w

Visually estimated intensities: s = strong, m = medium, w = weak.
[a] Sample coming directly from synthesis (precipitated powder).
[b] Sample crystallized isothermally at the indicated temperatures and subsequently quenched to room temperature.

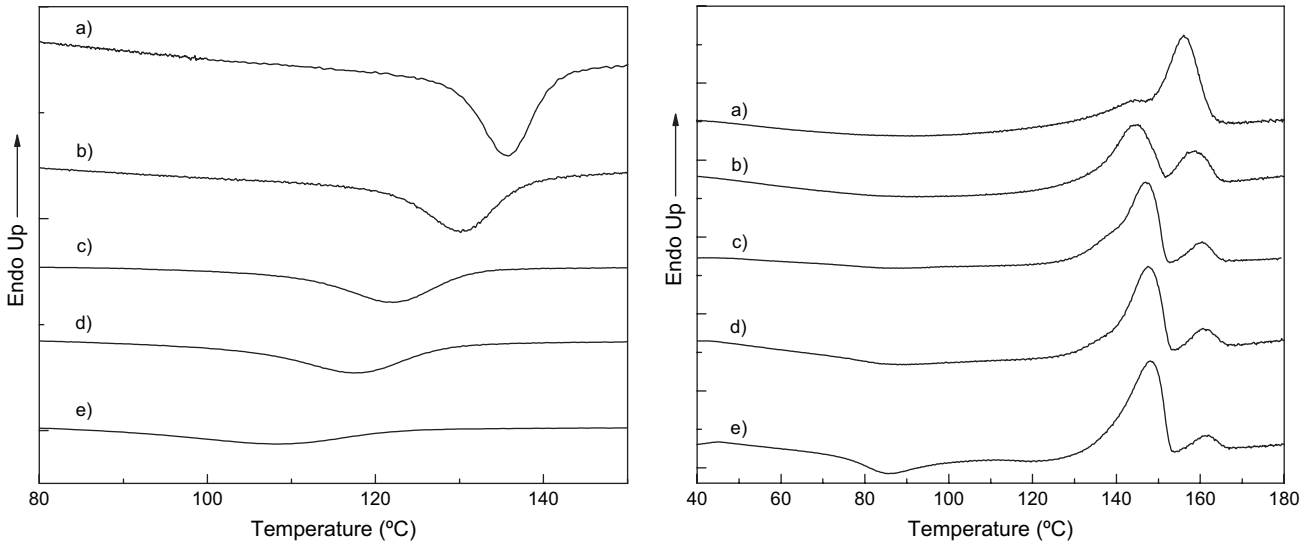

Fig. 5. DSC traces of nonisothermal crystallization of PAALM-1(HMW). Left: cooling traces at rates of 2.5 °C/min (a), 5 °C/min (b), 10 °C/min (c), 20 °C/min (d), and 40 °C/min (e). Right: heating traces of samples crystallized as previously indicated.

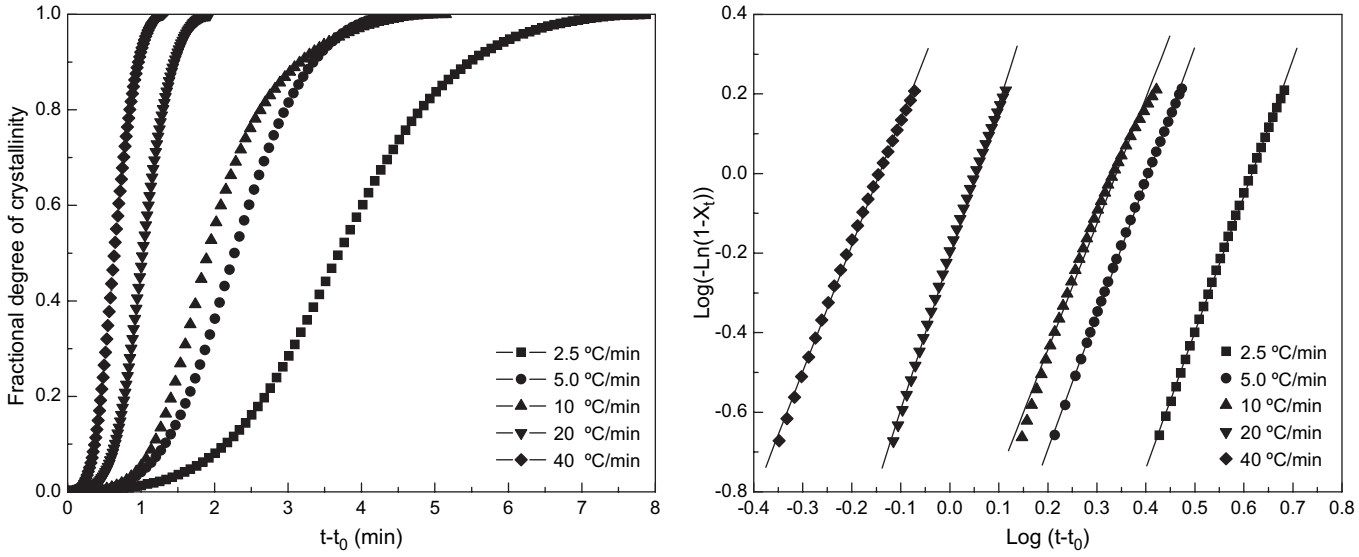

Fig. 6. Fractional degree of crystallinity vs time (left) and of plot of $\mathrm{Log}(-\mathrm{Ln}(1-X_t))$ vs $\mathrm{Log}(t-t_0)$ (right) for the nonisothermal crystallization of PAALM-1(HMW) at different cooling rates.

peak temperature and enthalpy steadily decreased at increasing cooling rates. The crystallized samples invariably show a double melting peak, the higher temperature component being almost insensitive to crystallization rate whereas the lower temperature one is observed to move up for increasing cooling rates. The evolution of fractional crystallinity X_c with crystallization time and the corresponding logarithmic graphs built according to the Avrami theory adapted for nonisothermal crystallization are shown in Fig. 6 and the thermal parameters resulting from this analysis are summarized in Table 3. Results indicate that crystallization of PAALM-1 was depressed at high crystallization rates and that the process took place by a mechanism that fits satisfactorily the Avrami prediction [14] with an exponent n close to 3 and K values steadily increasing with the cooling rate.

Table 3
Nonisothermal crystallization parameters for PAALM-1(HMW)

Φ(°C/min)[a]	2.5	5	10	20	40
n[b]	3.42	3.37	3.16	3.84	3.17
K (min^{-1})[b]	0.0061	0.043	0.085	0.63	2.81
$t_{1/2}$ (min)[c]	3.76	2.27	1.91	1.06	0.64
$t_{1/2}$ (min)[d]	3.99	2.28	1.94	1.02	0.64
T_c (°C)[e]	136	130	122	117	108
ΔH_c (J/g)[e]	37.5	27.1	26.7	29.1	19.7
T_m (°C)[f]	144/156	144/159	147/160	147/161	148/162
ΔH_m (J/g)[f]	47.7	24.8	33.3	32.9	38.6

[a] Cooling rate.
[b] Parameters of Avrami equation: $\mathrm{Ln}(1-X_c)=Kt^n$.
[c] Crystallization half-time determined experimentally.
[d] Crystallization half-time calculated by Avrami, $t_{1/2}=(\mathrm{Ln}\,2/K)^{1/n}$.
[e] Crystallization temperature and enthalpy.
[f] Melting temperature and enthalpy.

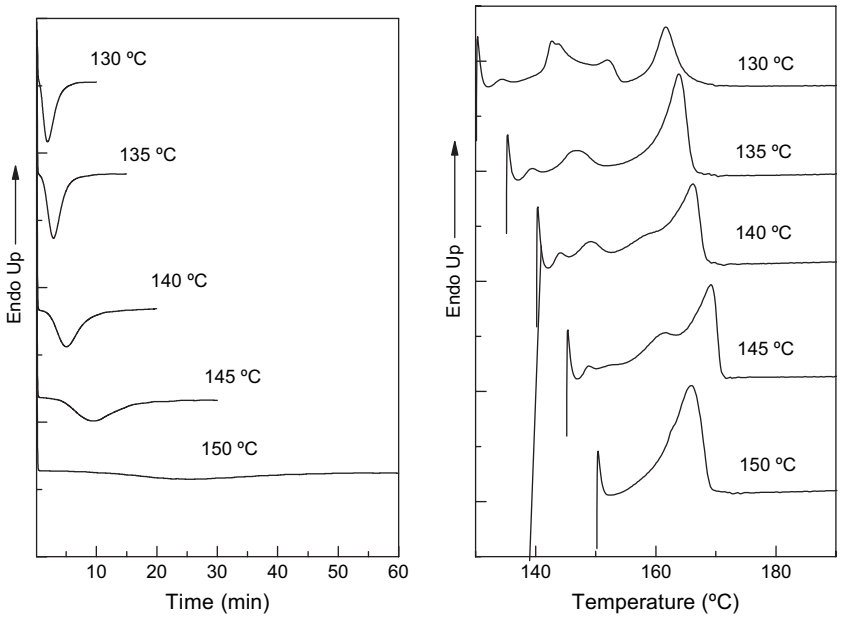

Fig. 7. Isothermal crystallization traces of PAALM-1(HMW) at the indicated temperatures (left) and heating traces (right) of the respective crystallized samples.

3.4. Isothermal crystallization

The isothermal crystallization of PAALM-1(HMW) was studied within the temperature range of 130–150 °C. The crystallization and fusion traces recorded along this study are shown in Fig. 7. A complex melting behaviour was observed for samples crystallized at lower temperatures ($T_c = 130$–140 °C) whereas a single endothermal peak was observed for those obtained at higher temperatures ($T_c = 145$ and 150 °C). Since the heating traces were recorded from the crystallization temperature uncontrolled nonisothermal crystallization of the material should be reasonably discarded. The multiple melting displayed by the material crystallized at low temperature must be therefore due, at least in part, to the presence of the two crystal forms and their interconversion happening upon heating (this point will be further discussed below). Fractional crystallinity as a function of time and the corresponding logarithmic Avrami plots for a relative crystallinity range of 0.2–0.8 are plotted in Fig. 8, and both experimental and calculated crystallization parameters are given in Table 4. As expected, crystallization rate decreased with crystallization temperature as it is clearly reflected by the regular increasing of crystallization half-times that is observed for increasing values of T_c. Avrami exponent values were found to oscillate between 2.1 and 2.7, which are rather low values for a spherulitic crystallization as is observed to happen in PAALM-1. Arguments based on soft-impingement or anisotropic growing of relative stiff polymers have been invoked in the specialized literature to explain the occurrence of such low n values [15].

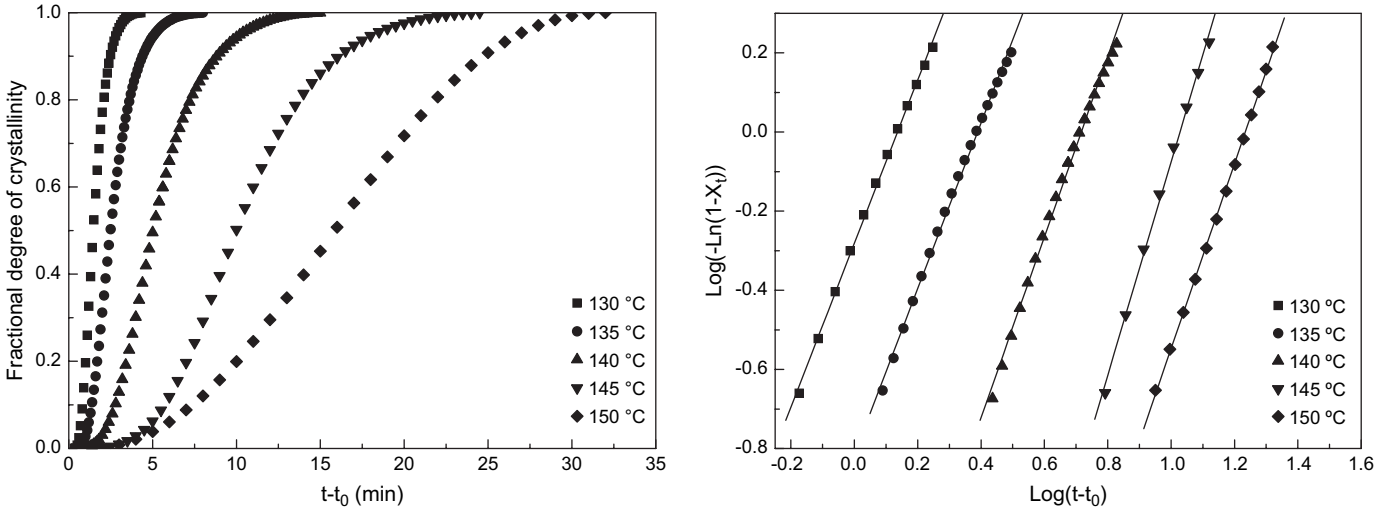

Fig. 8. Fractional degree of crystallinity vs time (left) and plot of Log(−Ln(1 − X_t)) vs Log($t - t_0$) (right) for isothermal crystallization of PAALM-1(HMW).

Table 4
Isothermal crystallization parameters for PAALM-1(HMW)

T_c (°C)[a]	130	135	140	145	150
n[b]	2.06	2.09	2.28	2.69	2.33
K (min^{-1})[b]	0.52	0.15	2.3×10^{-2}	1.7×10^{-3}	1.3×10^{-3}
$t_{1/2}$ (min)[c]	1.43	2.53	5.0	10.03	15.93
$t_{1/2}$ (min)[d]	1.14	2.07	4.41	9.36	14.75
$(t - t_0)$ (min)[e]	4	7.53	14.33	22.69	30.92
ΔH_c (J/g)[f]	21	25	35	34	34
T_m (°C)[g]	143/161	146/163	159	163	162
ΔH_m (J/g)[g]	28/8	18/13	44	43	35
G (μm/min)[h]	0.204	0.066	0.035	0.015	0.010

[a] Crystallization temperature.
[b] Parameters of Avrami equation: $\mathrm{Ln}(1 - X_c) = Kt^n$.
[c] Crystallization half-time determined experimentally.
[d] Crystallization half-time calculated by Avrami, $t_{1/2} = (\mathrm{Ln}\, 2/K)^{1/n}$.
[e] Crystallization onset time.
[f] Crystallization enthalpy.
[g] Melting temperature and enthalpy.
[h] Radial growth rate.

POM observations revealed that crystallization occurred instantaneously and that spherulites were formed for the whole range of assayed temperatures. The radial spherulite growth rate was monitored for several crystallization temperatures within the 130–150 °C range. As it can be seen in Fig. 9, an almost linear dependence as a function of time was observed for the spherulitic radius. The growth rate, which is given by the straight line slope, increased as crystallization temperature T_c decreased. The isothermal spherulitic crystallization behaviours of high and low molecular weight PAALM-1s are compared in Fig. 10. Temperatures approximately 50 °C lower were required for the low molecular weight homologous to crystallize and, at difference with the high molecular one, crystallization could be observed within both diffusion and nucleation controlled regions. The morphological analysis of crystallized films revealed that, for a similar spherulitic crystallization rate the number of growing spherulites was much larger for PAALM-1(HMW) than for PAALM-1(LMW),

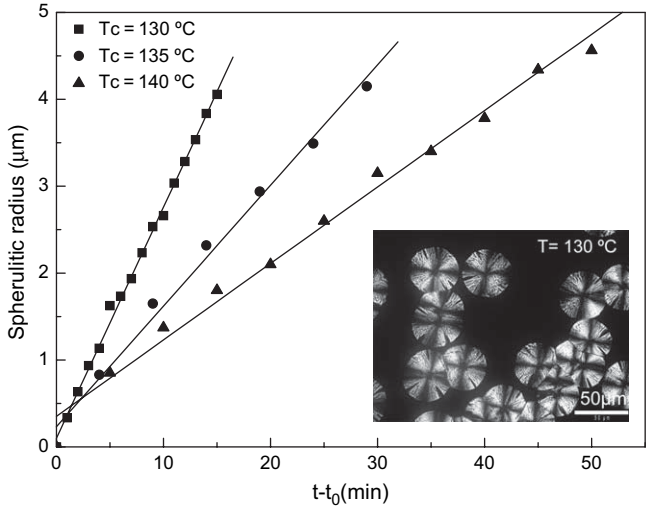

Fig. 9. Isothermal crystallization of PAALM-1(HMW). Spherulitic radius vs time at different crystallization temperatures. Inset: spherulites crystallized at 130 °C.

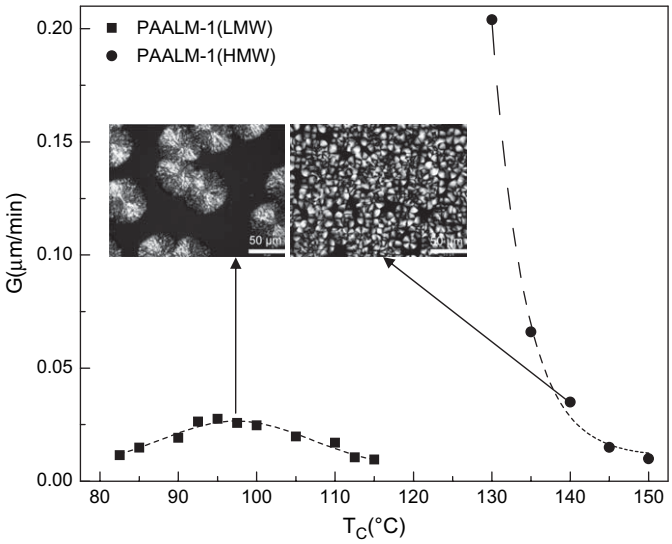

Fig. 10. Spherulitic radial growth rate as a function of the crystallization temperature for PAALM-1(LMW) and PAALM-1(HMW). Inset: spherulitic morphologies for PAALM-1(LMW and HMW) grown at similar radial crystallization rates.

suggesting that this may be the reason for the lower overall crystallization rate observed for the latter case by DSC.

3.5. Interconversion of crystal forms

The occurrence of two crystal forms in PAALM-1(HMW) in relation to its crystallization kinetics, both under isothermal and nonisothermal conditions, deserves particular attention. As indicated above, the X-ray analysis showed that the two melting peaks appearing in the samples crystallized from the melt corresponded to forms I and II. A comparative inspection of the thermograms registered for the kinetic study indicates that the presence of form II (higher temperature melting peak) was notably favoured by high crystallization temperatures and slow crystallization rates. Thus, samples made almost exclusively of this form could be obtained under favourable conditions such as isothermal crystallization at 150 °C and nonisothermal crystallization at 2.5 °C/min. On the contrary, form I (lower temperature melting peak) invariably appears contaminated with considerable amounts of form II suggesting that it partially converts into the latter by melting-recrystallization. This interpretation was confirmed by following the change in the relative areas of the two melting peaks as a function of the heating rate. As clearly seen in Fig. 11a, a notable decreasing of the higher temperature peak was observed as the heating rate increased. On the other hand, the relative area of the second peak largely increased when the sample was annealed at a temperature near below the melting temperature of the first peak (Fig. 11b). X-ray diffraction confirmed that transition from form I to form II was involved in the conversion of the lower temperature peak into the higher one (Fig. 11c). Nevertheless, the Avrami kinetics did not appear significantly altered by the occurrence of this crystal dimorphism indicating that forms I and II must be probably

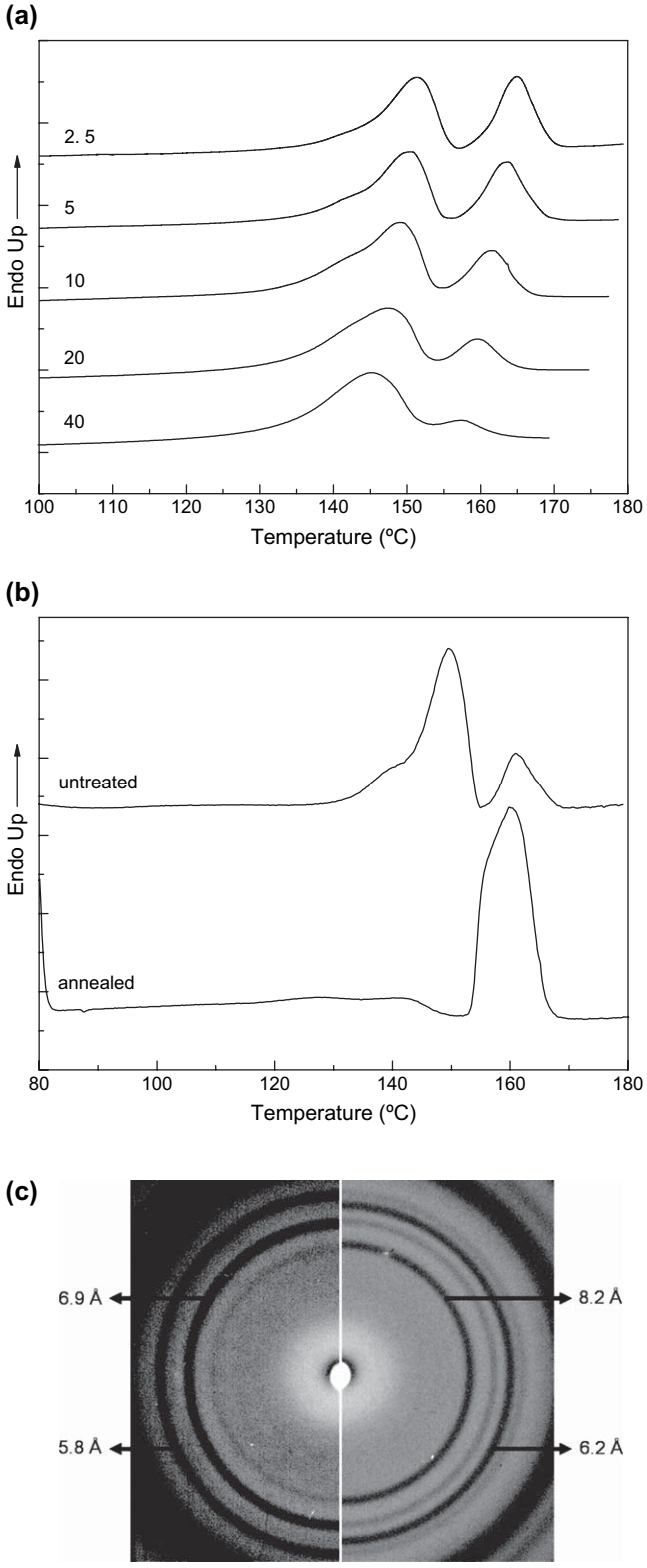

Fig. 11. DSC and WAXS analysis of a sample of PAALM-1(HMW) crystallized from the melt at 10 °C/min. (a) DSC traces recorded at the indicated heating rates (°C/min). (b) Compared DSC traces for the untreated sample and the sample annealed at 152 °C for 2 h. (c) Powder X-ray diffraction pattern of the untreated (left) and the annealed (right) samples.

crystallized by a similar mechanism, which is in agreement with the structural proximity that seems to exist between them.

4. Conclusion

The reaction of poly(β,L-malic acid) with diazomethane in acetone allows a complete methylation of the carboxyl side groups without significant cleavage of the polyester main chain. A poly(α-methyl β,L-malate) of $M_n \sim 25{,}000$ could be prepared by this method. This poly(malate) with increased molecular weight has structural and thermal behaviours significantly different from that displayed by its low molecular weight homologous. In contrast to PAALM-1(LMW), two crystal forms have been detected for PAALM-1(HMW). They are found in varying relative amounts depending on crystallization conditions. The isothermal and nonisothermal crystallization kinetics have been analyzed and found to fit the Avrami approach. Crystallization happens rapidly with the formation of well defined spherulites, the rate being severely limited by diffusion when performed under isothermal conditions at high undercooling. Crystallization of PAALM-1(HMW) is a highly nucleated process that explains the higher crystallization rate observed in the bulk for this polymer as compared to PAALM-1(LMW).

Acknowledgements

Financial support for this work was provided by CICYT (Spain) with grant MAT2003-06955-C02. Authors are indebted to AGAUR for the Ph.D. grant awarded to Carlos E. Fernández.

References

[1] Lee BS, Vert M, Holler E. Water-soluble aliphatic polyesters: poly(malic acid)s. In: Doi Y, Steinbuechel A, editors. Biopolymers. Polyester I, vol. 3a. Weinheim: Wiley-VCH; 2002. p. 75.
[2] Vert M. Polym Degrad Stab 1998;59:169.
[3] Bong-Seop L, Fujita M, Khazenzon NM, Wawrowsky KA, Wachsmann-Hogiu S, Farkas DL, et al. Bioconjugate Chem 2006;17:317.
[4] Portilla JA, García-Alvarez M, Martínez de Ilarduya A, Holler E, Muñoz-Guerra S. Biomacromolecules 2006;7:161.
[5] Kajiyama T, Kobayashi H, Taguchi T, Kataoka K, Tanaka J. Biomacromolecules 2004;5:169.
[6] Vert M, Lenz RW. ACS Polym Preprints 1979;20:608.
[7] Braud C, Vert M. Trends Polym Sci 1993;3:57.
[8] Fernández CE, Mancera M, Holler E, Galbis JA, Muñoz-Guerra S. Macromol Biosci 2005;5:172.
[9] Holler E. Poly(malic acid) from natural sources. In: Cheremisinoff NP, editor. Handbook of engineering polymeric materials. New York: Marcel Dekker; 1997. p. 93.
[10] Portilla JA, García-Alvarez M, Martínez de Ilarduya A, Muñoz-Guerra S. submitted for publication.
[11] Grassie N, Murria EJ, Holmes PA. Polym Degrad Stab 1984;6:47.
[12] Organ SJ, Barham PJ. J Mater Sci 1991;26:1368.
[13] Pazur RJ, Hocking PJ, Raymond S, Marchessault RH. Macromolecules 1998;31:6585.
[14] Avrami M. J Chem Phys 1939;7:1103.
[15] Cheng SZ, Wunderlich B. Macromolecules 1988;21:3328.